DOI https: //doi. org/10.1007/s11595-019-2144-5

# A New Type of Nanogel Carrier based on Mixed Pluronic Loaded with Low-Dose Antitumor Drugs

**YIN Meizhen[1,2], SU Zhenhong[1], CUI Bingcun[1], HAN Yingchao[3], DAI Honglian[3], YU Xin[1*]**

*(1. School of Medicine, Hubei Polytechnic University, Huangshi 435003, China; 2. School of Medicine, Inner Mongolia University for Nationalities, Inner Mongolia Tongliao 028000, China; 3. State Key Laboratory of Advanced Technology for Materials Synthesis and Processing, and Biomedical Materials and Engineering Center, Wuhan University of Technology, Wuhan 430070, China)*

**Abstract:** To design a new type of antitumor nanodrug carrier with good biocompatibility, a drug delivery system with a 2.19% drug-loading rate, measured by high-performance liquid chromatography (HPLC), was prepared by membrane hydration using a mixed polymer: Pluronic® F-127, which binds folic acid (FA), Pluronic® F-68 and triptolide (TPL) (FA-F-127/F-68-TPL). As a control, another drug delivery system based on a single polymer (FA-F-127-TPL) with a 1.90% drug-loading rate was prepared by substituting F-68 with F-127. The average particle sizes of FA-F-127/F-68-TPL and FA-F-127-TPL measured by a particle size analyzer were 30.7 nm and 31.6 nm, respectively. Their morphology was observed by atomic force microscopy (AFM). The results showed that FA-F-127-TPL self-assembled into nanomicelles, whereas FA-F-127/F-68-TPL self-assembled into nanogels. An MTT assay showed that a very low concentration of FA-F-127/F-68-TPL or FA-F-127-TPL could significantly inhibit the proliferation of multidrug-resistant (MDR) breast cancer cells (MCF-7/ADR cells) and induce cell death. The effects were significantly different from those of free TPL ($P < 0.01$). Using the fluorescent probe Nile red (Nr) as the drug model, FA-F-127/F-68-Nr nanogels and FA-F-127-Nr nanomicelles were prepared and then incubated with human hepatocarcinoma (HepG2) and MCF-7/ADR cells, and the fluorescence intensity in the cells was measured by a multifunctional microplate reader. The results indicated that both FA-F-127/F-68-Nr and FA-F-127-Nr had sustained release in the cells, but HepG2 and MCF-7/ADR cells exhibited significantly higher endocytosis of FA-F-127/F-68-Nr than that of FA-F-127-Nr ($P < 0.01$). A nude mice transplanted tumor model was prepared to monitor FA-F-127/F-68-Nr in the tumor tissue and organs by whole-body fluorescent imaging. The results showed that FA-F-127/F-68-Nr targeted tumor tissues. The prepared nanogels had small particle size, were easy to swallow, exhibited slow release property, targeted tumor cells, and could improve the antitumor effects of TPL; hence, they are ideal carriers for low-dose antineoplastic drugs.

**Key words:** pluronic; nanogels; nano drug carriers; triptolide

## 1 Introduction

Nanocarriers are particularly important in tumor therapy because of their high permeability and retention in solid tumors. Liposomes, polymer carriers (*eg*, micelles, hydrogels, polymer vesicles, dendritic molecules, and nanofibers), carbon nanomaterials (*eg*, nanotubes and graphene), inorganic nanoparticles (*eg*, silicon particles), and hybrid and other nanomaterials are used for drug transport[1]. Some drug carrier materials in *vivo* tend to cause issues such as kidney toxicity or mismatched normal cells because of the lack of biodegradability and targeting of the diseased site, whereas liposomes or polymer carriers can enhance the solubility of drugs, slow down drug clearance, reduce tumor resistance, and enhance the efficacy of drugs.

Polymer nanogels with sensitivity to the external environment are of great interest in biomedical material research. Drug carrier materials used in the preparation of polymer nanogels include polyacrylic acid, polyacrylamides, grandonucleosides, polysaccharides, and other synthetic polymers with hydrophilic functional groups. Polymer nanogels are of two types: chemical cross-linked gels and physical cross-linked gels[2].



(Received: Feb.13, 2018; Accepted: Apr. 12, 2018)

YIN Meizhen(尹美珍): Prof.; Ph D; E-mail: yxjun0758@163.com

*Corresponding author: YU Xin(喻昕):Prof.; E-mail: yuxinwjh@163.com

Funded by the National Natural Science Foundation of Hubei Province (No. 2014CFB306), the National Natural Science Foundation of China(No. 51772233), the National Key Research and Development Program of China (No. 2016YFC1101605) and the Science and Technology Support Program of Hubei Province (No. 2015BAA085)

Chemical cross-linking using a cross-linking agent and initiator induces toxicity, makes thoroughly cleaning of the gel difficult, or it damages cells or tissues because of the use of radiation. Physical cross-linked gels are prepared under mild conditions without chemical reactions and are therefore more conducive to biomedical application. Pluronic inhibits drug efflux by the membrane transporter P-glycoprotein (P-gp) associated with multidrug resistance[3-6] and is therefore used as a nanogel in tumor therapy research. To enhance the antitumor effect of chemotherapy drugs, Jonug *et al*[7] prepared a heparin-Pluronic F-127 (heparin-F-127) nanogel for the delivery of hydrophobic drugs paclitaxel and deoxyribonuclease. Kim *et al*[8] prepared a chitosan-modified Pluronic F-68 (F-68) nanogel to deliver gold nanorods and chlorin e6 photosensitizer by photo-cross-linking. In the experiment, the drug carrier system showed good antitumor effects in *vivo* and in *vitro*.

The aim of this study was to prepare nanodrug carriers using Pluronic selected due to its easy-to-modify and self-assembling properties, study their physicochemical and biological properties in order to obtain new formulations for antitumor drugs.

## 2 Experimental

### 2.1 Preparation of a drug delivery system based on polymers

2.1.1 Folic acid-Pluronic F-127 conjugate

The required amount of folic acid (FA; Aladdin) was dissolved in dimethyl sulfoxide (DMSO); equimolar amounts of *N*,*N*'-carbonyldiimidazole (CDI) were added; the mixture was stirred in the dark and left to react for 24 h. Then, one-fourth amount of F-127 (BASF, Ludwigshsfen, Germany) was added, and the mixture was again left to react in the dark for 24 h. The mixture was then put in a dialysis bag (Spectra, Millipore, MWCO 1000) and dialyzed against purified water for 72 h. The purified water was replaced at intervals of 3-6 h and then lyophilized to obtain an FA-F-127 conjugate.

2.1.2 Drug delivery system loading TPL

The polymer drug delivery system was prepared by membrane hydration. FA-F-127 and F-68 (BASF, Ludwigshsfen, Germany), 100 mg each, and 10 mg of triptolide (TPL; Aladdin), selected as a carrier material, were dissolved in absolute ethanol. The solution was subjected to nitrogen stream, and the mixture was vacuum-dried overnight, forming a transparent film. This was followed by hydration at 50 ℃ using a thermostatic shaker with 15 mL of deionized water for 2 h thermostatic shaker. After cooling to room temperature, the suspension was centrifuged at 10,000 rpm for 10 min, and the supernatant was filtered through a sterile 0.22 μm cellulose acetate filter to obtain an FA-F-127/F-68-TPL solution. The carrier material was replaced with 100 mg each FA-F-127 and F-127 to obtain an FA-F-127/TPL solution. Two blank carrier solutions were obtained using 100 mg each of FA-F-127 and F-68 or 100 mg each of FA-F-127 and F-127 in the absence of the TPL.

All the prepared solutions could be lyophilized for storage. Reversed-phase high-performance liquid chromatography (RP-HPLC) was used to determine the TPL content in the FA-F-127/F-68-TPL and FA-F-127/TPL solutions.

2.1.3 Drug delivery system loading Nile red

To facilitate the detection of the biological properties of the drug-loaded polymer, FA-F-127-Nr and FA-F-127/F-68-Nr were prepared by the same method outlined in Section 2.1.2 using the hydrophobic fluorescent probe Nile red (Nr) (HPLC, Aladdin) instead of TPL as the drug model. Ultraviolet-visible (UV-vis) spectrophotometry was used to determine the Nr content in the FA-F-127-Nr and FA-F-127/F-68-Nr solutions.

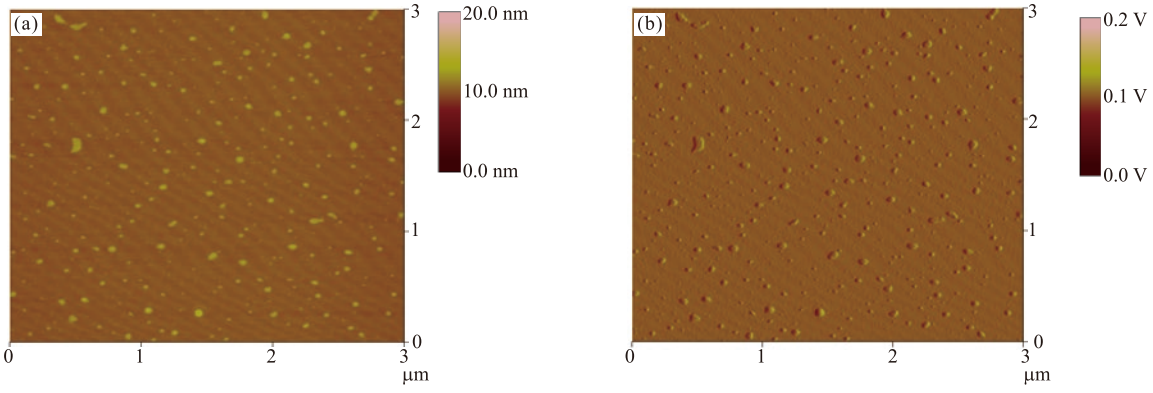


Fig.1 The AFM images showing the morphology of FA-F-127-TPL colloidal particles

### 2.2 Observation of the morphology

The morphology of FA-F-127/F-68-TPL and FA-F-127-TPL was observed, and atomic force microscopy (AFM) images were captured by a Bruker atomic force microscopy (BioScopy Catalyst, USA).

### 2.3 Determination of particle size

The particle size of FA-F-127/F-68-TPL and FA-F-127-TPL was measured using a Zetasizer Nano dynamic light scattering system (Malvern, Worcestershire, UK).

### 2.4 Cell culture

Human hepatocarcinoma (HepG2) cells (CCTCC) were cultured with Roswell Park Memorial Institute (RPMI) 1640 Medium (Gibco) supplemented with 10% fetal bovine serum (FBS; Gibco), and doxorubicin-induced multidrug-resistant (MDR) breast cancer cells (MCF-7/ADR cells; Dr. Wang's group at the University of Science and Technology of China) were cultured with RPMI 1640 Medium supplemented with 10% FBS and 5 μg/mL doxycycline (DOX; GR, Aladdin) at 37 ℃ in a 5% $CO_2$ incubator (NU-4500E, Nuaire Inc., Plymouth, MN, USA).

### 2.5 MTT assay

MCF-7/ADR cells in the logarithmic growth phase were seeded in 96-well culture plates at a cell density of $5 \times 10^4$. After the cells were incubated for 24 h, the culture medium was replaced in the drug groups with the complete medium containing 25, 50, and 100 ng/mL (according to TPL calculation) of FA-F-127-TPL, FA-F-127/F-68-TPL, and free TPL, respectively; in the blank carrier group, with the complete medium containing the corresponding concentration of FA-F-127 or FA-F-127/F-68; and in the blank control group, with only the fresh medium.

All cells were cultured in the incubator. After the cells of each group were treated for 24, 48, 72, and 96 h, respectively. The absorbance values were measured by an MTT assay using a multifunctional microplate reader (SpectraMax Paradigm, Molecular Devices, USA).

### 2.6 Cell endocytosis

HepG2 cells in the logarithmic growth phase were seeded in 96-well culture plates. After 24 h of inoculation, the culture medium was replaced in the experimental group with the complete medium containing 0.4, 0.2, and 0.1 μg/mL (according to Nr calculation) of FA-F-127-Nr and F-127/F-68-Nr, respectively; in the blank carrier group, with the complete culture medium containing F-127/F-68 or FA-F-127 with the corresponding carrier concentration; and in the blank control group, with only the fresh complete medium.

The cells of each group were incubated for 2 h, and the culture medium was discarded. The cells were washed three times with phosphate-buffered saline (PBS), and then 150 μL of DMSO was added to each well. After shaking the plate at 300 rpm for 30 min, the fluorescence intensity of the cells in each well was measured (excitation wavelength 552 nm; emission wavelength 650 nm) using the multifunctional microplate reader.

### 2.7 Intracellular drug release

MCF-7/ADR cells in the logarithmic growth phase were inoculated in 96-well culture plates. The cells were cultured for 24 h. The culture medium was replaced in the experimental group with the complete medium containing 0.5 μg/mL (according to Nr calculation) of FA-F-127-Nr and FA-F-127/F-68-Nr,respectively; in the blank carrier group, with the complete culture medium containing FA-F-127/F-68 and FA-F-127 with the corresponding carrier concentration; and in the blank control group, with only the fresh complete medium.

After incubation for 2 h, the culture medium of each group was removed, the cells were washed three times with PBS, and a serum-free medium was added. The cells of each group were cultured in the incubator for 0, 1, 2, 4, 6, and 24 h, respectively; the cells were washed and dissolved using the method described in Section 2.6; and the fluorescence intensity of each well was measured by the multifunctional microplate reader.

### 2.8 Targeting *in vivo*

A nude mice subskin model transplanted with human hepatocarcinoma cells was prepared to observe the targeting function of FA-F-127/F-68 on tumor tissue. The mice were randomly divided into two groups ($n$ = 6). In the experimental group, 0.2 mL of FA-F-127/F-68-Nr at a concentration of 0.5 μg/mL was injected from the tail vein of each mouse; in the control group, the corresponding volume of normal saline was given to each mouse. After injection for 2 h, the mice in the two groups were sacrificed, and the subcutaneous tumor tissue, heart, liver, spleen, lungs, kidneys, and pancreas were immediately removed. The aggregation and distribution of drugs in the tumor tissues and the organs and tumor tissue were measured using a whole-body fluorescent imaging system (IVIS® Lumina XRMS Series III).

### 2.9 Statistics

All the experimental data were presented as an average with standard deviation ($\bar{x} \pm s$), and the significance of the mean difference was examined using

Student's *t*-test.

# 3 Results and discussion

## 3.1 Appearance of the drug delivery system

AFM images show FA-F-127-TPL as tiny spherical particles in the monodisperse state (Figs.1(a), and 1(b)) and FA-F-127/F-68-TPL as flat, spherical particles with a network structure (Figs.2(a), 2(b)). Occasionally, two or more particles were close together (as indicated by the arrow). This shows that FA-F-127-TPL self-assembled into nanomicelles, whereas FA-F-127/F-68-TPL self-assembled into a polymer nanogel.

Pluronic is an amphiphilic triblock copolymer comprising hydrophilic polyoxyethylene (POE) and hydrophobic polyoxypropylene (PPO), which can self-assemble into nanomicelles in aqueous solutions. Because Pluronic can be easily modified, and researchers have developed a large number of targeted nanodrug-loaded micelles based on Pluronic. Nguyen *et al*[9] prepared folate-modified F-127-DOX micelles. The FA-F-127-TPL prepared in this experiment was in the form of nanomicelles. Hydrophilic or amphiphilic polymers containing multifunctional groups can form nanogels with a 3D network structure by physical or chemical cross-linking[10,11]. Sasaki Y *et al*[12] argued that polymer chains can form nanogels via physical cross-linking by means of noncovalent interactions (including hydrogen bonds, van der Waals forces, hydrophobic forces, host-guest interactions, and electrostatic interactions). F-127 or F-68 is commonly used to prepare nanogels[13]. The FA-F-127/F-68-TPL prepared in this experiment was a nanogel, which may be formed by physical cross-linking. Therefore, FA-F-127 and F-127 together can self-assemble into nanomicelles and with F-68 can self-assemble to form a nanogel.

## 3.2 Particle size of the drug delivery system

Figs.3(a) and 3(b) show that the average particle size of FA-F-127-TPL was 31.6 nm and the particle size range was 15.7-68.6 nm; FA-F-127/F-68-TPL had two average particle sizes, 30.7 nm and 80.3 nm, and two corresponding particle size ranges, 13.5-43.8 nm, with 82.2% particles and 50.7-122.8 nm with 17.8% particles.

AFM images showed that the particles of FA-F-127-TPL are monodisperse. However, FA-F-127/F-68-TPL contains a small number of particles next to one another. We speculated that the particle size range of 50.7-122.8 nm may be the reason, which may be related to the amount of water in the gel solution. Studies have shown that the physical and chemical properties of nanocarriers, such as particle size and hydrophobicity, influence their enhanced permeability and retention (EPR) effect. To achieve efficient drug delivery, nano-

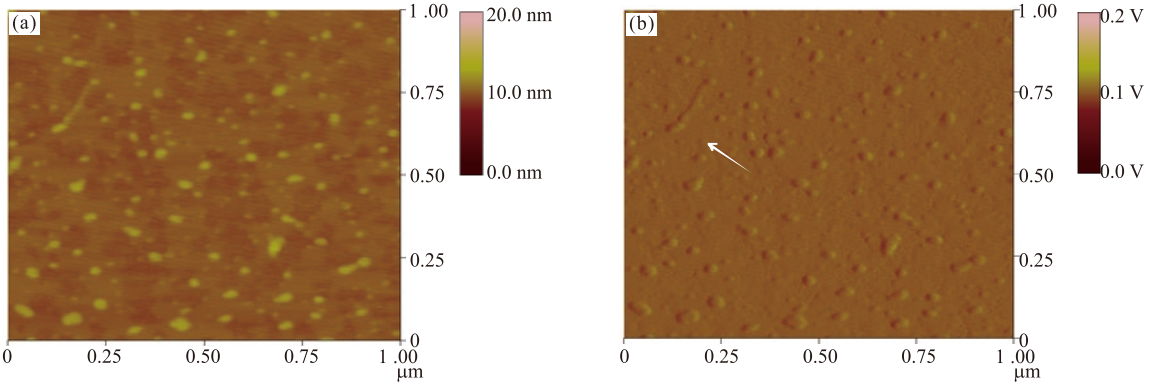


Fig.2 The AFM images showing the morphology of FA-F-127/F-68-TPL colloidal particles

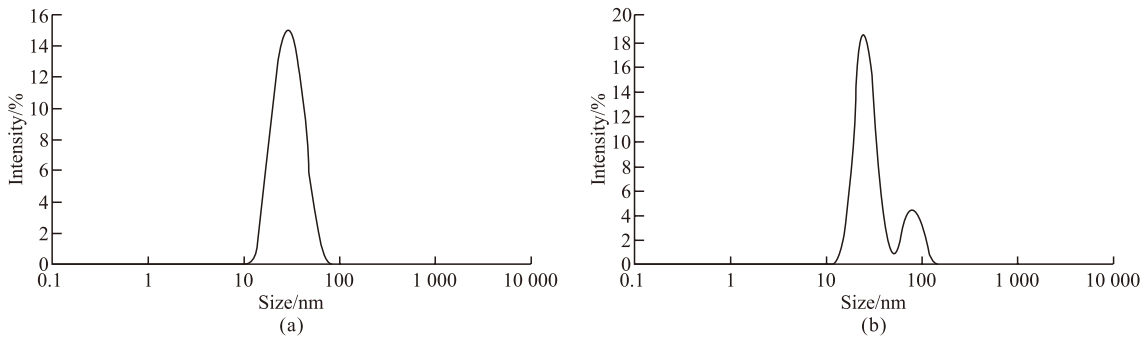


Fig.3 Size distribution of FA-F-127-TPL and FA- F-127/F-68-TPL colloidal particles: (a) FA-F-127, (b) FA-F-127/F-68

carriers need to have good long-circulating characteristics in order to avoid mononuclear macrophages, liver and kidney metabolism[14] so that nanodrugs can penetrate the tumor site via the blood vessels[15]. Nanoparticles less than 100 nm in size have better EPR[16,17]. The FA-F-127/F-68-TPL nanogels prepared in this experiment had good long-circulating characteristics and an enhanced EPR effect due to good stability, strong dilution resistance, small particle size, and good hydrophilicity.

### 3.3 Drug-loading rate of the drug delivery system

The drug-loading rate of FA-F-127/F-68-TPL was 2.19%, whereas that of FA-F-127-TPL was 1.90%. Therefore, the drug-loading rate of nanogels was slightly higher than that of nanomicelles.

To improve the drug-loading rate, we prepared a variety of drug carriers. Compared with drug carriers having a drug-loading rate of 10% or more reported in the literature, and even graphene carriers with a drug-loading rate of up to 80%, the nanogel prepared in this experiment had a low drug-loading rate. This may seem to be a disadvantage for a drug carrier but is actually an advantage for TPL, doxorubicin, paclitaxel, and other drugs. The reason is that for a drug with a strong antitumor effect, the dose administered is extremely low, which means that the drug formulation needs to be diluted. The low drug-loading rate can reduce the dilution and avoid the problem of poor stability due to dilution. In addition, with a low drug-loading rate, the drug carrier concentration is relatively high, increasing the stability of the nanogel and enhancing the dilution *in vivo*.

### 3.4 Toxic effects of the drug delivery system on tumor cells

The optical density (OD) values in Table 1 indicate that compared with the control group, and the two empty carrier groups had no significant effect on the proliferation of MCF-7/ADR cells ($P > 0.05$). In addition, the treatment of cells with FA-F-127/F-68-TPL, FA-F-127-TPL, and free TPL with different TPL concentrations for 24-96 h significantly inhibited the proliferation of MCF-7/ADR cells ($P < 0.01$) and with extended treatment, gradually induced cell death. However, the effect of FA-F-127/F-68-TPL and FA-F-127–TPL was significantly enhanced compared with free TPL ($P < 0.01$). This shows that FA-F-127/F-68-TPL and FA-F-127-TPL can significantly improve the antitumor effect of TPL.

In recent years, studies have shown that TPL plays a significant role in inhibiting proliferation of the cell and inducting cell apoptosis[18-21], showing strong antitumor activity in a number of malignant tumors. There are many molecular targets for TPL in a large number of tumor cells. As mentioned earlier, Pluronic inhibits the drug efflux of P-gp associated with multidrug resistance. Alakhova *et al* and Song *et al* demonstrated that Pluronic can inhibit the activity of the P-gp drug pump by reducing intracellular adenosine triphosphate (ATP) levels and increase the accumulation of the P-gp substrate in MDR cells [22,5]. Therefore, as a carrier material, Pluronic can have a synergistic effect on MDR tumors.

**Table 1 OD value of each group after treating MCF-7/ADR cells for 24-96 h ($\bar{x} \pm s$, $n = 8$)**

| Groups | Dose /(ng/mL) | OD | | | |
|---|---|---|---|---|---|
| | | 24 h | 48 h | 72 h | 96 h |
| Control | 0 | 0.3633 ± 0.015 | 0.4472 ± 0.014 | 0.4823 ± 0.010 | 0.5198 ± 0.013 |
| FA-F-127 | 0 | 0.3605 ± 0.021 | 0.4398 ± 0.013 | 0.4776 ± 0.019 | 0.5205 ± 0.018 |
| FA-F-127/F-68 | 0 | 0.3583 ± 0.022 | 0.4400 ± 0.015 | 0.4678 ± 0.015 | 0.5180 ± 0.028 |
| TPL | 25 | 0.3283 ± 0.019$^{A}$ | 0.4322 ± 0.017 | 0.4292 ± 0.018$^{A}$ | 0.3850 ± 0.005$^{A}$ |
| | 50 | 0.3102 ± 0.021$^{A}$ | 0.4315 ± 0.012$^{A}$ | 0.3903 ± 0.023$^{A}$ | 0.3533 ± 0.018$^{A}$ |
| | 100 | 0.2690 ± 0.012$^{A}$ | 0.3803 ± 0.016$^{A}$ | 0.2745 ± 0.027$^{A}$ | 0.2338 ± 0.020$^{A}$ |
| FA-F-127-TPL | 25 | 0.2836 ± 0.017$^{A,B}$ | 0.2802 ± 0.017$^{A,B}$ | 0.2890 ± 0.011$^{A,B}$ | 0.2743 ± 0.021$^{A,B}$ |
| | 50 | 0.2809 ± 0.014$^{A,B}$ | 0.2758 ± 0.018$^{A,B}$ | 0.2431 ± 0.010$^{A,B}$ | 0.1902 ± 0.020$^{A,B}$ |
| | 100 | 0.2505 ± 0.017$^{A,B}$ | 0.2545 ± 0.018$^{A,B}$ | 0.2125 ± 0.016$^{A,B}$ | 0.1591 ± 0.019$^{A,B}$ |
| FA-F-127/F-68-TPL | 25 | 0.2772 ± 0.019$^{A,B}$ | 0.2792 ± 0.016$^{A,B}$ | 0.2858 ± 0.018$^{A,B}$ | 0.2615 ± 0.022$^{A,B}$ |
| | 50 | 0.2722 ± 0.015$^{A,B}$ | 0.2608 ± 0.008$^{A,B}$ | 0.2242 ± 0.006$^{A,B}$ | 0.1732 ± 0.018$^{A,B}$ |
| | 100 | 0.2405 ± 0.015$^{A,B}$ | 0.2400 ± 0.022$^{A,B}$ | 0.1985 ± 0.018$^{A,B}$ | 0.1490 ± 0.013$^{A,B}$ |

$^{A}$Compared with the control group; $P < 0.01$; $^{B}$ Compared with the TPL group; $P < 0.01$; OD, optical density

**Table 2 Fluorescence intensity values of HepG2 cells in each group ($\bar{x} \pm s$, $n = 8$)**

| Groups | Fluorescence intensity | | |
|---|---|---|---|
| | 0.1 μg/mL | 0.2 μg/mL | 0.4 μg/mL |
| Control | 180336 ± 28056 | | |
| FA-F-127 | 183032 ± 29640 | 177597 ± 31127 | 183024 ± 24830 |
| FA-F-127/F-68 | 168671 ± 24006 | 191583 ± 14979 | 174742 ± 32315 |
| FA-F-127-Nr | 360848 ± 49643* | 417982 ± 29819* | 674221 ± 53006* |
| FA-F-127/F-68-Nr | 435090 ± 69246*# | 535655 ± 53936*# | 906395 ± 145469*# |

* Compared with the control group; $P < 0.01$; #Compared with the FA-F-127-Nr group; $P < 0.01$

**Table 3 Fluorescence intensity and drug content in MCF-7/ADR cells of each group at different times**

| Groups | Fluorescence intensity | | Content | |
|---|---|---|---|---|
| | FA-F-127/F-68-Nr | FA-F-127-Nr | FA-F-127/F-188-Nr | FA-F-127-Nr |
| 0 h | 796627 ± 55280** | 606950 ± 44140 | 100% | 100% |
| 1 h | 633215 ± 16677* | 535630 ± 27256 | 79.48% | 88.25% |
| 2 h | 538287 ± 31573 | 477548 ± 10895 | 67.57% | 78.68% |
| 4 h | 496969 ± 12874** | 423250 ± 8194 | 62.38% | 69.73% |
| 6 h | 473557 ± 6855** | 351344 ± 21750 | 59.45% | 57.89% |
| 24 h | 403011 ± 20937* | 325129 ± 24562 | 50.59% | 53.57% |

Compared to the FA-F-127-Nr group, *$P < 0.05$ and ** $P < 0.01$

### 3.5 Endocytosis of the drug delivery system by tumor cells

Table 2 shows the fluorescence intensity values of each group determined after HepG2 cells were treated with FA-F-127/F-68-Nr and FA-F-127-Nr for 2 h. There was no significant difference in the fluorescence intensity between the two blank carrier groups and the control group ($P > 0.05$), indicating that the two blank vectors did not produce fluorescence. The fluorescence intensity was significantly higher in both FA-F-127/F-68-Nr and FA-F-127-Nr groups than in the blank control group ($P < 0.01$) (the higher the drug concentration, the stronger the fluorescence intensity) and was significantly higher in the FA-F-127/F-68-Nr group than in the FA-F-127-Nr group ($P < 0.01$). This indicated that the tumor cells show strong endocytosis of FA-F-127/F-68-Nr nanogels and FA-F-127-Nr nanomicelles, but the endocytosis of FA-F-127/F-68-Nr nanogels is easier.

Endocytosis is the main pathway of cell uptake of macromolecules in extracellular media. Depending on the size of the swallowed matter and the mechanism of uptake, endocytosis is of three types: phagocytosis, pinocytosis, and receptor-mediated endocytosis. HepG2 cells have overexpressed folate receptors and thus, in this study, ingested a large amount of FA-F-127/F-68-Nr through either phagocytosis or receptor-mediated endocytosis.

Studies have reported that the morphology of nanocarriers has an effect on tumor therapy. The length-to-width ratio of nanomaterials can affect their interaction with cells (such as uptake), circulating time in the body, and penetrating ability in the tumor[23]. Therefore, depending on the morphology of colloidal particles, there are significant differences in the uptake of FA-F-127/F-68-Nr and FA-F-127-Nr by HepG2 cells. It is possible that flat, spherical particles have greater contact with the cells than spherical particles, resulting in a greater probability of forming receptor-ligand complexes and therefore easier phagocytosis and ingestion through receptor-mediated endocytosis.

### 3.6 Slow releasing action of the drug delivery system in cells

The fluorescence intensity values (subtracting background fluorescence) of the cells in each group are shown in Table 3. The concentration of FA-F-127/F-68-Nr in MCF-7/ADR cells was significantly higher than that of FA-F-127-Nr ($P < 0.01$) after incubation with the cells for 2 h. With an increase in the time of incubation, the concentration of Nr in the two groups gradually decreased. Although even after 24 h, it was still more than 50% and the content of FA-F-127/F-68-Nr was still significantly higher than that of FA-F-127-Nr ($P < 0.01$). This indicated the rate of endocytosis of FA-F-127/F-68-Nr is faster than that of FA-F-127-Nr, and there might be a certain degree of metabolism and/or efflux of Nr in tumor cells after ingestion. In addition, the slow decrease in intracellular Nr also indicated that

FA-F-127/F-68-Nr and FA-F-127-Nr have the same sustained release properties in the cells.

### 3.7 Tumor tissue-targeting function of drug-loaded nanogels

After 2 h of injection, in the FA-F-127/F-68-Nr group, there was strong fluorescence in the tumor tissue but either weak or no fluorescence was observed in the liver, spleen, lungs, kidneys, and pancreas (see Fig.4(a)). In the FA-F-127/F-68 blank vector group, there was no or weak fluorescence in the tumor tissue and in the liver, spleen, lungs, kidneys, and pancreas (see Fig.4(b)). It can be seen that FA-F-127/F-68-Nr is targeted to tumor tissue in vivo.

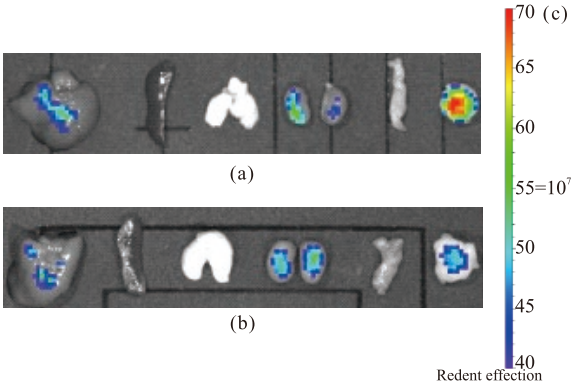


Fig.4 Fluorescence imaging of tumor tissues and organs after 1 h of intravenous injection. (a) The FA-F-127/F-68-Nr group. (b) The FA-F-127/F-68 group. (c) The color from top to bottom indicates the fluorescence intensity level. Red indicates the strongest fluorescence, while blue indicates the weakest fluorescence

Folate receptors are highly conserved in normal tissues and are overexpressed on most tumor cell membranes, such as in kidney cancer, ovarian cancer, lung cancer, breast cancer, and colon cancer. Because of folate receptor-mediated endocytosis, follicular receptors on tumors have been used for targeted delivery of anticancer drugs, genes, and radiopharmaceuticals. FA is a small-molecule vitamin, essential to the human body, and folate receptors exhibit high affinity. FA-F-127/F-68-TPL nanogels specifically recognize the folate receptors of tumor cells, showing tumor tissue-targeting function.

## 4 Conclusions

In this study, we used membrane hydration to prepare FA-F-127-TPL nanomicelles and FA-F-127/F-68-TPL nanogels. Results indicated that FA-F-127/F-68-TPL and FA-F-127-TPL significantly inhibit the proliferation of MCF-7/ADR MDR cells at a low concentration (25 ng/mL), which can significantly improve the antitumor effect of drugs. Although the antitumor effect of FA-F-127/F-68-TPL and FA-F-127-TPL is not significantly different, the results of experiment with Nr as the drug model indicated that HepG2 and MCF-7/ADR cells show stronger uptake of FA-F-127/F-68-Nr nanogels than of FA-F-127-Nr nanomicelles, indicating that an increased uptake of drug-loading nanogels can improve the bioavailability of drugs in tumor cells. Moreover, nanogels have better stability than nanomicelles, and thus, can resist higher dilution in vivo. The prepared drug-loaded nanogels had a small particle size and good hydrophilicity. Therefore, nanogels are better than nanomicelles as drug carriers.

Results of the experiment on the nude mice transplanted tumor model showed that the nanogels were mainly distributed in the tumor tissue, confirming their apparent targeting of tumor tissue. Also, the nanogels had good sustained release in the MCF-7/ADR cells. In addition, the preparation of nanogels is simple; no chemical cross-linking agent is used; Pluronic has good biocompatibility, can be removed by the kidneys, and does not accumulate in other important organs. The mechanism of reversal of tumor multidrug resistance can play a synergistic effect on the drug being loaded. Therefore, even if nanogels have a low drug-loading rate, they are ideal carriers for highly active antitumor drugs and specifically and efficiently transport the loaded drugs to the tumor site through the best pharmacokinetic process in order to achieve safe, reliable, and efficient treatment.

### References

[1] Li Y, Maciel D, Rodrigues J, *et al*. Biodegradable Polymer Nanogels for Drug/Nucleic Acid Delivery[J]. *Chemical Reviews,* 2015, 115: 8 564-8 608

[2] Sina N, Hugh R, Joselito M, *et al*. Progress Toward Robust Polymer Hydrogels[J]. *Australian Journal of Chemistry*, 2011, 64: 1 007-1 025

[3] Song CK, Balakrishnan P, Shim CK *et al*. Enhanced in vitro Cellular Uptake of P-gp Substrate by Poloxamer-modified Liposomes (PMLs) in MDR Cancer Cells[J] *Journal of Microencapsulation,* 2011, 28: 575-581

[4] Hanke U, May K,Rozehnal V, *et al*. Commonly Used Nonionic Surfactants Interact Differently with the Human Efflux Transporters ABCB1（p-glycoprotein）and ABCC2 (MRP2)[J]. *European Journal of Pharmaceutics and Biopharmaceutics*, 2010,76: 260-268

[5] Li WN, Sun JL, Guan QX, *et al*. Research Progress of Pluronic as a Drug Delivery System for Reversing Multidrug Resistance of Tumors[J]. *Chinese Pharmaceutical Journal*, 2016,51:1 270-1 273

[6] Mu L Q, Hu X B, Hu YY, *et al*. Advances in the Study of Overcoming

Multidrug Resistance in Cancer by Pluronic Block Copolymers[J]. *Chinese Journal of Hospital Pharmacy*, 2014, 34: 1 780-1 784

[7] Joung YK, Jang JY, Choi JH, *et al*. Heparin-Conjugated Pluronic Nanogels as Multi-Drug Nanocarriers for Combination Chemotherapy-[J]. *Molecular Pharmaceutics,* 2013, 10: 685-693

[8] Kim JY, Choi WI, Kim M, *et al*. Tumor-targeting Nanogel That Can Function Independently for Both Photodynamic and Photothermal Therapy and Its Synergy from the Procedure of PDT Followed by PTT[J]. *Journal of Controlled Release*, 2013, 171: 113-121

[9] Nguyen DH, Lee JS, Bae JW, *et al*. Targeted Doxorubicin Nanotherapy Strongly Suppressing Growth of Multidrug Resistant Tumor in Mice[J]. *International Journal of Pharmaceutics*, 2015, 495: 329-335

[10] Merino S, Martín C, Kostarelos K, *et al*. Nanocomposite Hydrogels: 3D Polymer-Nanoparticle Synergies for On-Demand Drug Delivery[J]. *ACS Nano*, 2015, 9: 4 686-4 697

[11] Ahmed E M. Hydrogel: Preparation, Characterization, and Applications: A Review[J]. *Journal of Advanced Research*, 2015, 6: 105-121

[12] Sasaki Y, Akiyoshi K. Nanogel Engineering for New Nanobiomaterials: from Chaperoning Engineering to Biomedical Applications[J]. *Chemical Record*, 2010, 10: 366-376

[13] Zhou QY, Zhang ZH, Pan J F, *et al*. Development of Poloxamers Used as Carriers for New Dosage Forms of Hydrophobic Drugs[J]. *Chinese Journal of Modern Applied Pharmacy*, 2011, 28: 315-319

[14] Longmire M, Choyke PL, Kobayashi H. Clearance Properties of Nano-sized Particles and Molecules as Imaging Agents: Considerations and Caveats[J]. *Nanomedicine,*2008, 3: 703-717

[15] Zhao P, Zheng M, Yue C, *et al*. Improving Drug Accumulation and Photothermal Efficacy in Tumor Depending on Size of ICG Loaded Lipid-Polymer Nanoparticles[J]. *Biomaterials*, 2014, 35: 6 037-6 046

[16] Perrault SD, Walkey C, Jennings T, *et al*. Mediating Tumor Targeting Efficiency of Nanoparticles Through Design[J]. *Nano Letters*, 2009, 9: 1 909-1 915

[17] Lee H, Fonge H, Hoang B, *et al*. The Effects of Particle Size and Molecular Targeting on the Intratumoral and Subcellular Distribution of Polymeric Nanoparticles[J]. *Molecular Pharmaceutics,* 2010, 7: 1 195-1 208

[18] Tao Y, Zhang ML, Ma PC, *et al*. Triptolide Inhibits Proliferation and Induces Apoptosis of Human Melanoma A375 Cells[J]. *Asian Pacific Journal of Cancer Prevention*, 2012, 13: 1 611-1 615

[19] Li H, Hui L, Xu W, *et al*. Modulation of P-glycoprotein Expression by Triptolide in Adriamycin-Resistant K562/A02 Cells[J]. *Oncology Letters*, 2012, 3: 485-489

[20] Clawson K A, Borja-Cacho D, Antonoff M B, *et al*. Triptolide and TRAIL Combination Enhances Apoptosis in Cholangiocarcinoma[J]. *Journal of Surgical Research*, 2010, 163: 244-249

[21] Johnson SM, Wang X, Evers BM. Triptolide Inhibits Proliferation and Migration of Colon Cancer Cells by Inhibition of Cell Cycle Regulators and Cytokine Receptors[J]. *Journal of Surgical Research*, 2011, 168: 197-205

[22] Alakhova DY, Rapoport NY, Batrakova EV, *et al*. Differential Metabolic Responses to Pluronic in MDR and Non-MDR Cells: A Novel Pathway for Chemosensitization of Drug Resistant Cancers[J]. *Journal of Controlled Release ,* 2010, 142: 89-100

[23] Agarwal R, Jurney P, Raythatha M, *et al*. Effect of Shape, Size, and Aspect Ratio on Nanoparticle Penetration and Distribution inside Solid Tissues Using 3D Spheroid Models[J]. *Advanced Healthcare Materials*, 2015, 15: 2 269-2 280